MAGNETIC RESONANCE IN MEDICINE

Quantitative Measurements of Cerebral Blood Flow in Rats using the FAIR Technique: Correlation with Previous Iodoantipyrine Autoradiographic Studies

Nikolaos V. Tsekos, Fangyi Zhang, Hellmut Merkle, Masao Nagayama, Costantino Iadecola, Seong-Gi Kim

Flow-sensitive alternating inversion recovery (FAIR) is a recently introduced MRI technique for assessment of perfusion that uses blood water as an endogenous contrast agent. To characterize the FAIR signal dependency on spin tagging time (inversion time (TI)) and to validate FAIR for cerebral blood flow (CBF) quantification, studies were conducted on the rat brain at 9.4 T using a conventional gradient-recalled echo sequence. The T_1 of cerebral cortex and blood was found to be 1.9 and 2.2 s, respectively, and was used for CBF calculations. At short TIs (<0.8 s), the FAIR signal originates largely from vascular components with fast flows, resulting in an overestimation of CBF. For TI > 1.5 s, the CBF calculated from FAIR is independent of the spin tagging time, suggesting that the observed FAIR signal originates predominantly from tissue/capillary components. CBF values measured by FAIR with TI of 2.0 s were found to be in good agreement with those measured by the iodoantipyrine technique with autoradiography in rats under the same conditions of anesthesia and arterial pCO_2. The measured pCO_2 index on the parietal cortex using the FAIR technique was 6.07 ml/100 g/min per mmHg, which compares well with the pCO_2 index measured by other techniques. The FAIR technique was also able to detect the regional reduction in CBF produced by middle cerebral artery occlusion in rats.

Key words: cerebral blood flow; perfusion; hypercapnia; MRI.

INTRODUCTION

Recent advances have demonstrated that, instead of using exogenous flow tracers, arterial blood tagged by RF pulses can be used as an *endogenous* flow tracer. Arterial spin tagging has been performed by continuous inversion of inflowing spins in the neck area (1, 2). The tagged blood water spins move into capillaries and exchange with tissue water spins. The signal difference between images with and without spin tagging is directly related to tissue blood flow. The continuous tagging method can provide accurate quantification of cerebral blood flow (CBF) changes in rats with altered CO_2 levels (2, 3). However, in human studies, the transit time of tagged blood spins is long, resulting in significant signal loss of the tagged spins due to T_1 relaxation of spins traveling into the imaging slice (4). Also, long pulses for continuous spin tagging create magnetization transfer effects, reducing signals by as much as 70% when a single coil is used for both spin preparation and imaging (3). Although the use of two coils can eliminate magnetization transfer effects, the coil position for spin tagging is limited to the neck, resulting in a long travel distance of spins from the neck to the imaging slice (5).

An alternative method is to obtain spin tagging by a short pulse. The echo-planar imaging and signal targeting with alternating RF (EPISTAR) and flow-sensitive alternating inversion recovery (FAIR) techniques belong to this category (6–9). Similar to the continuous inversion method, EPISTAR uses inverted spins on the inferior side of the imaging slice as a flow tracer. In the FAIR technique, slice-selective (flow-sensitive) and non-slice-selective (flow-insensitive control) inversion recovery (IR) images are obtained. The difference of two IR images is directly related to tissue blood flow (7). Absolute CBF during resting conditions has been measured in rats and humans (8–10), and relative CBF changes have been determined during task-induced neural activity (7, 10–12). However, these pulsed tagging methods have not been validated for accurate CBF measurements.

The aims of this study are (a) to evaluate the contrast mechanism in terms of the spin tagging time used between the inversion pulse and the image acquisition, (b) to determine whether the FAIR method (with a *single* inversion time) is able to detect regional difference in resting CBF and the increases in CBF produced by different levels of hypercapnia, and (c) to determine whether FAIR can detect the CBF reductions secondary to focal cerebral ischemia. All FAIR studies were performed on a rodent model at 9.4 T.

METHODS

FAIR Technique

The FAIR technique requires the collection of two IR images: one with slice-selective IR (ssIR) and the other with non-slice-selective IR (nsIR) (7). After the slice-selective inversion pulse, the fully relaxed inflowing blood spins enter the imaging slice during the spin tagging time and exchange with tissue spins. As a consequence, the tissue magnetization M_{ss} relaxes with a flow-dependent *apparent* T_1 (T_{1app}); i.e., $1/T_{1app} = 1/T_1 + f/\lambda$, where f is the CBF in units of ml blood/g tissue/s and λ is

MRM 39:564–573 (1998)

From the Center for Magnetic Resonance Research, Departments of Radiology (N.V.T., H.M., S.-G.K.) and Neurology (F.Z., M.N., C.I.), University of Minnesota Medical School, Minneapolis, Minnesota.

Address correspondence to: Seong-Gi Kim, CMRR, University of Minnesota Medical School, 385 East River Road, Minneapolis, MN 55455.

Received June 9, 1997; revised October 16, 1997; accepted October 17, 1997.

This work was supported by Grants RR08079, NS32437 (S-G. K., N.V.T.), NS31318 (C.I.), NS34179 (C.I., F.Z., M.N.), and NS35806 (C.I., F.Z., M.N.) from the National Institutes of Health, and grants from the Whitaker Foundation (S-G. K), W. M. Keck Foundation, and the University of Minnesota (S-G. K). C.I. is an established investigator of the American Heart Association.

0740-3194/98 $3.00

the blood-tissue partition coefficient (1, 2). The nsIR image serves as a "control" image since the magnetization (M_{ns}) of both the tissue and blood, after the global inversion pulse, relax with T_1. The FAIR image (ΔM) is defined as the subtraction of M_{ns} from M_{ss} (7, 8, 12–14). The ΔM at any inversion time (TI) is given by

$$\Delta M \equiv M_{ss} - M_{ns} = 2M_o \mathrm{TI} \frac{f}{\lambda} e^{-\mathrm{TI}/T_1} \kappa(\mathrm{TI}, T_1, T_{1b}) \quad [1]$$

where M_o is the fully relaxed magnetization and κ(TI, T_1, T_{1b}) is a correction factor. In cases in which blood and tissue water have different T_1 values, the correction factor κ(TI, T_1, T_{1b}) is $\kappa(t, T_1, T_{1b}) = [1 - \exp(-\gamma t)]/\gamma t$ where $\gamma = 1/T_{1b} - 1/T_1$ and T_{1b} is the T_1 of arterial blood water. When blood and tissue water spins have the same T_1 values, $\kappa = 1.0$. Equation [1] is based on the following assumptions: (a) the nsIR is flow independent, (b) there is no contribution of magnetization from vessels with fast flow or the "macrovascular" compartment, (c) enough time is allowed for the spins that enter the inverted slice to distribute in the "microvasculature" compartment of the tissue, and (d) water is a freely diffusible tracer. Then, the FAIR signal ΔM is directly proportional to tissue blood flow. Regional CBF is defined as blood flow of tissue, including capillary.

From Eq. [1], CBF maps can be calculated from the FAIR image with an independent measurement of M_o and T_1 on a pixel-by-pixel basis. Both M_o and T_1 can be determined by standard fitting of nsIR images over inversion times. Arterial blood water T_1 (T_{1b}) was measured separately and the average value was used for all studies. The coefficient λ is assumed to be 0.9 ml/g (15) with uniform spatial distribution.

MRI Methods

All MR studies were conducted on a 9.4-T, 31-cm bore diameter horizontal magnet (Magnex, Abington, UK), interfaced to a Unity console (Varian, Palo Alto, CA). The system was equipped with an actively shielded 11-cm-diameter gradient insert (Magnex, Abington, UK), which operates at a maximum strength of 300 mT/m and a slew rate of 1000 mT/m/ms. A two-coil assembly was used for the FAIR studies; a volume coil (7-cm diameter, 13-cm length) was used for RF transmission (inversion and excitation), and a circular surface coil (2-cm diameter) was placed over the skull for signal reception. The coils were tuned at 400 MHz and geometrically decoupled from one another. For blood T_1 measurements, a smaller volume coil (5-cm diameter, 5-cm length) was used. Before imaging, the homogeneity of the magnetic field was manually optimized on a slab twice the thickness of the imaging slice.

In all imaging studies, a magnetization-prepared ultrafast gradient-recalled echo technique was used with centric phase-encoding steps (i.e., collecting the zero k-space encoding step first), RF spoiling, and phase-encoding gradient refocusing. The parameters used were TR = 3.3 ms, TE = 1.9 ms, flip angle = 22°, matrix size = 64 × 64, FOV = 2.5 × 2.5 cm^2, and slice thickness = 1 mm. With these parameters, the acquisition time per image was 212 ms.

For the FAIR studies, ssIR and nsIR images were collected sequentially. A delay time of 10 s was used between images to allow full relaxation of the longitudinal magnetization. An 8-ms-long adiabatic full passage with hyperbolic secant modulation and a R value of 16 was used to generate B_1-insensitive inversion (16), followed by a crushing gradient (20 ms long with 5 G/cm). The ssIR slab thickness was set to 1 cm to ensure inversion in the 1-mm-thick imaging slice and minimal perturbation from the imperfect edge of the inversion profile. The efficiency of adiabatic inversion pulses within the imaging slice is greater than 99%, which was verified experimentally and theoretically (16).

To measure brain T_1, nsIR images of the same slice for perfusion studies were acquired with 40 different TIs ranging from 0.1 to 20 s. It should be mentioned that, to obtain maximal signal-to-noise ratio (SNR), signal amplification was set higher in FAIR than in T_1 measurements, and thus, M_o determined from T_1 studies can not be used for CBF calculation. Instead, the M_o maps were calculated from the nsIR and T_1 maps, as described later.

MRI Protocols and Animal Models

This work was composed of four studies: (a) measurement of the blood T_1, (b) dependence of the FAIR signal on the inversion recovery time, (c) CBF measurements during graded hypercapnia, and (d) CBF reduction in focal ischemia secondary to occlusion of MCA. Different animal preparations, including anesthesia conditions, were used in each of these studies, as described under each specific protocol.

Measurement of Blood T_1

Male Sprague-Dawley (SD) rats weighing 250–300 g (n = 9) were anesthetized with a 1.5-ml/kg im injection of a 1:1:4 mixture of acepromazine (10 mg/ml), xylazine (20 mg/ml), and ketamine (100 mg/ml) (referred to as "ketamine mixture"). Arterial blood was withdrawn from the thoracic descending aorta, through an incision on the abdomen, and immediately transferred to heparinized tubes, which were then placed in the volume coil. The T_1 was measured with an IR spectroscopic sequence collecting 40 TI values between 0.1 and 20 s, with a 20-s delay after acquisition.

Dependence of FAIR Signal on TI

Male SD rats weighing 200–250 g (n = 6) were initially anesthetized with 1.5 ml/kg of the ketamine mixture and maintained under anesthesia with periodic injection of the same anesthetic (0.5 ml/kg/h). Eighteen pairs of ssIR and nsIR images were collected for each TI value, which ranged between 0.1 and 5 s.

Graded Hypercapnia Studies

Male SD rats weighing 250–300 g (n = 5) were initially anesthetized with 1–5% isoflurane (Abbott Labs, North Chicago, IL) in 100% oxygen. Then, the rats were surgically prepared with a tracheotomy for ventilation and cannulations of the femoral artery and vein. The venous line was used for intermittent delivery of tubocurarine (4 mg/kg) (Bristol Meyers Squibb, Princeton, NJ) and pancuronium bromide (1.25 mg/kg) (Gensia Pharmaceu-

tical, Irvine, CA). The arterial catheter was used for monitoring arterial blood pressure by a computerized polygraph system (Acknowledge, Biopak, CA) and arterial blood gases by a blood gas analyzer (Model 1304, Instrumentation Laboratory, Milano, Italy). After the surgical procedures were completed, isoflurane was discontinued and anesthesia was maintained with α-chloralose (100 mg/kg; iv; maintenance, 20 mg/kg/h) (Sigma, St. Louis, MO). In each animal, two to three different blood pCO_2 levels were attained and maintained by adjusting the stroke volume of the ventilator. Non-slice-selective IR images with variable TI were collected at basal pCO_2 conditions for generation of the T_1 map. For FAIR studies, TI was set to 2.0 s. At the basal pCO_2 state, 54 pairs of ssIR and nsIR images were collected. To reduce the total acquisition time, only ssIR images were collected during higher pCO_2 states.

Focal Cerebral Ischemia

Focal cerebral ischemia was produced by occlusion of the middle cerebral artery (MCA) in spontaneously hypertensive rats weighing 300–350 g ($n = 5$) (see ref. 17). The left MCA was exposed via a subtemporal approach and occluded either proximal ($n = 2$) or distal ($n = 3$) to the origin of the lenticulostriate arteries (17). MR studies were performed 3–96 h after the MCA occlusion. During MR studies, the animals were kept under anesthesia with the ketamine mixture as described in the Measurement of Blood T_1 section. The TI was set equal to T_1 of the normally perfused brain area to maximize FAIR signal. Twenty-six pairs of images were then averaged. In multislice studies, three to four slices with thickness of 1 mm and the center-to-center gap of 2 mm were sequentially collected.

Data Analysis

All data were processed by using STIMULATE (18) and PV-WAVE (Visual Numerics, Boulder, Colorado). All *k*-space data were Fourier-transformed in magnitude mode. From 40 nsIR images, T_1 maps were generated using a monoexponential least-squares fitting routine on a pixel-by-pixel basis (19). The M_0 maps were calculated from the corresponding nsIR images and T_1 maps by using $M_{ns}(TI) = M_0(1 - 2e^{-TI/T_1})$.

The FAIR images (ΔM) were generated by subtracting the nsIR from ssIR images in magnitude mode. For the hypercapnia studies, ΔM at elevated pCO_2 states ($\Delta M_{(CO_2)}$) was generated by subtracting the averaged $M_{ns(basal)}$, measured at basal pCO_2, from the $M_{ss(CO_2)}$ measured at elevated pCO_2, i.e., $\Delta M_{(CO_2)} = M_{ss(CO_2)} - M_{ns(basal)}$. CBF maps were determined on a pixel-by-pixel manner using Eq. [1] from the calculated ΔM and M_o, the measured T_1, and the blood tissue partition coefficient λ of 0.9 ml/g (15).

In all studies, two regions of interest (ROIs) were analyzed: the parietal cortex and the caudate putamen (CP). The average CBF (ml/100 g/min) was calculated within each ROI. To determine the relationship between CBF and pCO_2, the CBF from ROIs was plotted as a function of the corresponding pCO_2. The increase in CBF corresponding to each mmHg of arterial pCO_2 increase (CO_2 index; ml/100 g/min/mmHg) was provided by the slope of the regression line. Unless otherwise indicated, data are presented as mean ± SEM.

RESULTS

FAIR Imaging at 9.4 T

Results from a FAIR experiment conducted on a normal rat brain under ketamine anesthesia at 9.4 T are illustrated in the panel of images in Fig. 1. These images correspond to ssIR images collected with TI = 2 s (Fig. 1A), T_1 map (Fig. 1B), and FAIR images of a living rat (Fig. 1C) and the dead animal (Fig. 1D). All images were obtained in the same coronal slice. The anatomical ssIR image (Fig. 1A) demonstrates relatively good contrast of the distinct anatomical areas in the brain. A spatial T_1 map of tissue water protons from the rat brain at 9.4 T (Fig. 1B) was obtained from 40 nsIR images; the T_1 of the brain tissue ranged from 1.7 to 2.0 s. The average T_1 from eight animals was 1.91 ± 0.06 s SD for parietal cortex, 1.78 ± 0.10 s SD for CP, and 2.04 ± 0.05 s SD for the lateral ventricles and corpus callosum. In comparison, the average T_1 (T_{1b}) of arterial rat blood water proton at 9.4 T was 2.20 ± 0.07 s SD ($n = 9$).

The quality of the 64 × 64 FAIR image with TI of 2.0 s (Fig. 1C) and spatial resolution of 0.39 × 0.39 × 1.0 mm^3 allows for clear identification of anatomical areas that correspond to different CBF rates and T_1. It is evident that there is no observable FAIR signal from areas surrounding the brain, as compared to the anatomical images, since these areas correspond to the scalp and muscle tissue with no or very low perfusion. The large vessels, with substantially larger flow, as compared to the tissue vessels, can be easily identified as the high signal intensity areas. As an additional validation that the obtained FAIR signal is related to CBF, the animal was sacrificed. The FAIR image (Fig. 1D) of the dead animal shows no signal enhancement, as expected due to the complete lack of flow.

TI Dependence of FAIR

A panel of FAIR images of a representative rat collected at variable TI values (0.2, 0.4, 0.6, 0.8, 1.0, 1.4, 1.6, 2.0, and 5.0 s) is shown in Fig. 2. In the FAIR image with TI of 0.2 s (Fig. 2A), large FAIR signal enhancement was observed in *large* vessels, suggesting that the transit time of tagged spins into the imaging slice is fast. At low TI values (TI < 0.8 s), high FAIR contrast was observed primarily on the cortex, whereas the rest of the brain tissue demonstrates relatively reduced FAIR contrast. However, when increasing TI values (e.g., TI ≥ 1.0 s, Fig. 2E), the signal of the caudate putamen increased and approached the FAIR signal of the cortex. At a TI of 5 s, FAIR signal intensity decreased due to T_1 relaxation. It is noteworthy that *large vessels including large veins* have high FAIR contrast, even at longer TI values. After the slice-selective inversion pulse, these vessels are filled very quickly by fresh spins with fully relaxed magnetization, in a "wash-in" fashion. In contrast, after the global inversion pulse, all the inflowing spins experience the inversion pulse and relax with blood T_1. Consequently, there are large FAIR signals from the macrovasculature with high flows at all inversion times.

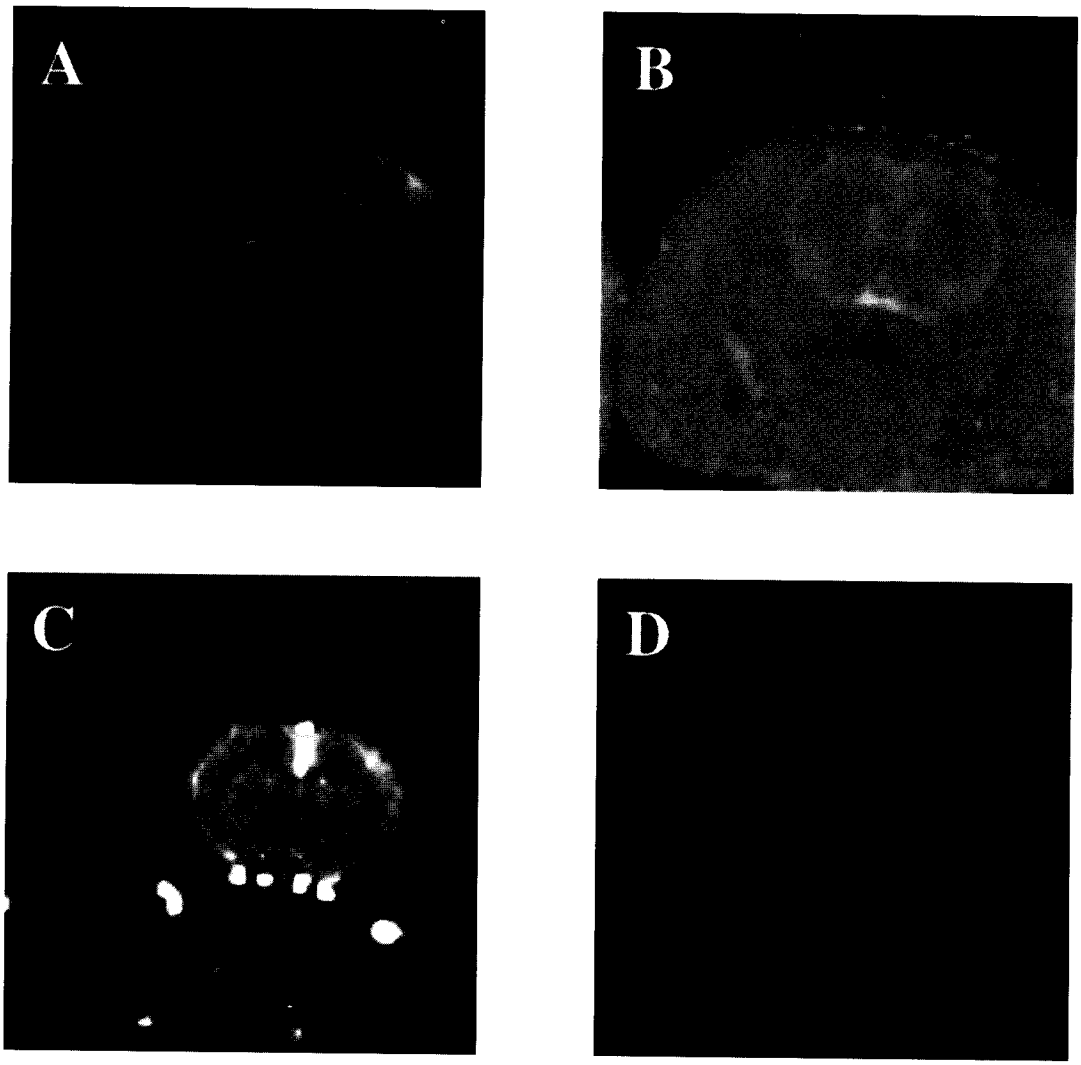

FIG. 1. Coronal images of a representative rat that consist of the ssIR image at TI = 2.0 s (A), the calculated T_1 map (B), the corresponding FAIR image with 0.39 × 0.39 mm in-plane resolution (C), and the FAIR image after the animal was sacrificed (D). The FAIR images (C, D) were collected at TI = 2.0 s. The high intensity spot in the middle of the IR image (A) is a DC artifact.

Data from three animals anesthetized by the ketamine mixture are illustrated in Fig. 3; the TI dependence of the FAIR signal normalized to M_o (Fig. 3A), and the corresponding calculated CBF (Fig. 3B) of an ROI placed on the cortex. Rectangles represent the animal shown in Fig. 2. Note that large vessels identified by high signal intensities at short TI were not included in the ROI. It is evident that the FAIR signal progressively increases as the TI increases until it reaches a broad plateau centered around TI $\approx T_1$. Then, FAIR signal is progressively reduced. This observation is consistent in all six animals. Such dependence is expected from Eq. [1] due to the competing mechanisms of the inflow of fresh spins and the longitudinal relaxation of the tissue, during the evolution period TI, which is consistent with previous simulations (13, 20). The TI dependence of CBF demonstrates that for TI > 1.5, the CBF is independent of the TI value as expected from Eq. [1], suggesting that the FAIR signal is mainly a perfusion component. However, at low TI values, the calculated CBF is both highly overestimated and TI dependent.

Graded Hypercapnia

In Fig. 4, the FAIR images (Figs. 4A, 4B, and 4C) and the corresponding CBF maps (Figs. 4D, 4E, and 4F) collected at pCO_2 = 25 mmHg (Figs. 4A and 4D), 40 mmHg (Figs. 4B and 4E), and 71 mmHg (Figs. 4C and 4F) are shown. Animals were anesthetized by α-chlorose. All images were collected with the TI of 2 s to ensure the acquisition of perfusion components. Increased signal enhancement was observed in the FAIR images collected at higher pCO_2 values. For example, the FAIR signal intensity at the parietal cortex increased 302% and 764% at pCO_2 of 40 and 71 mmHg, respectively, compared to the FAIR contrast for a hypocapnic condition (pCO_2 = 25 mmHg). The CBF calculated from the FAIR images on the parietal cortex was determined to be 22, 160, and 240 ml/100 g/min for pCO_2 values of 25, 40, and 71 mmHg, respectively. A similar trend was also observed for the CP. The average CBF calculated from five animals with the FAIR technique at normocapnia (pCO_2 = 38 ± 2 mmHg) was 91 ± 31 ml/100 g/min (n = 5) in parietal cortex and 83 ±

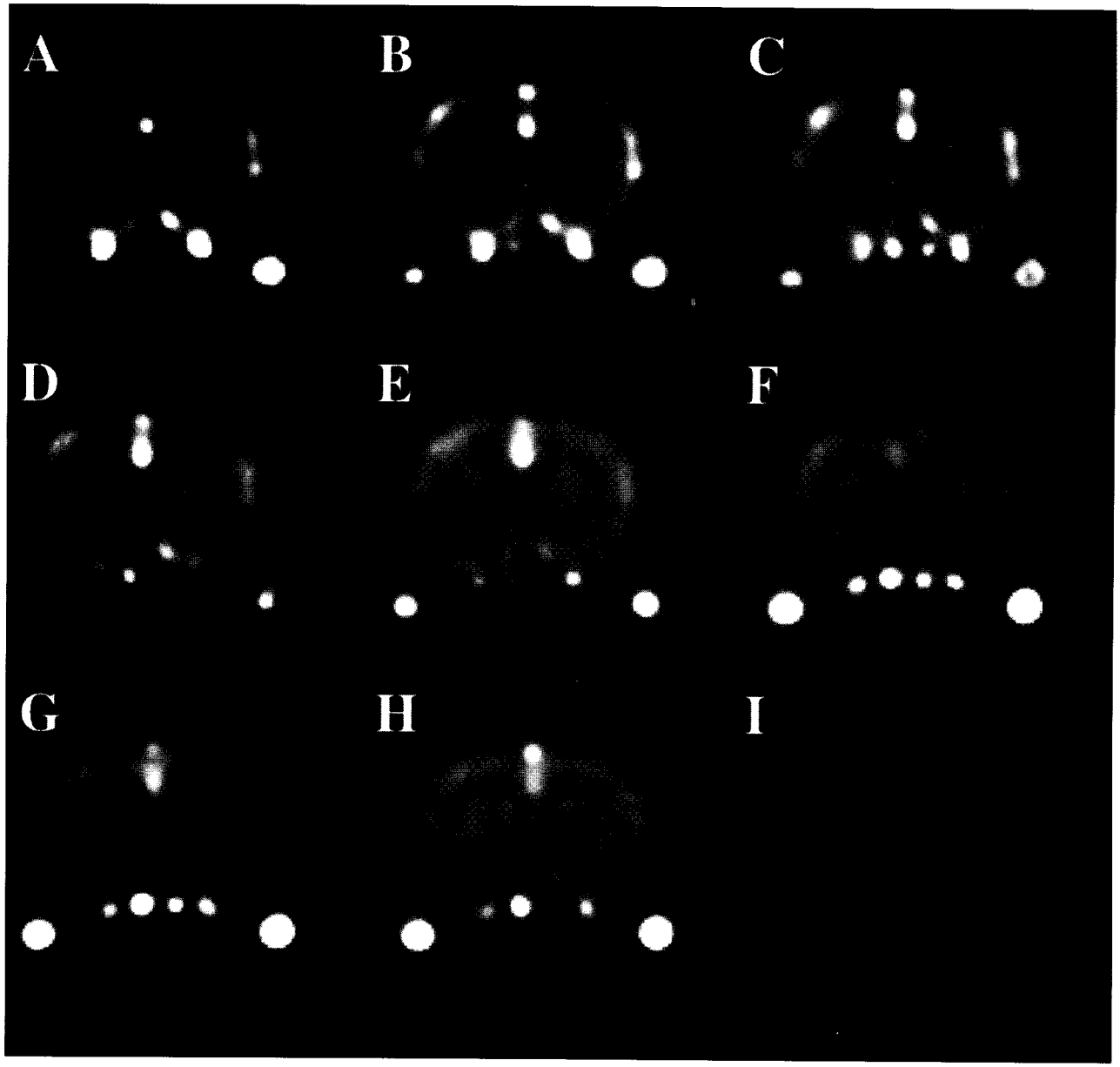

FIG. 2. A panel of nine coronal FAIR images of a representative rat, generated at different TI values: (A) 0.2 s, (B) 0.4 s, (C) 0.6 s, (D) 0.8 s, (E) 1.0 s, (F) 1.4 s, (G) 1.6 s, (H) 2.0 s, and (I) 5.0 s. A Gaussian filter with a full width at half height of a pixel was applied to improve the visualization of the FAIR contrast.

30 ml/100 g/min (n = 5) in the CP. With hypercapnia (pCO_2 = 65 ± 5 mmHg), CBF increased to 243 ± 54 ml/100 g/min (n = 6, one animal was measured at two pCO_2 levels) in the parietal cortex and to 221 ± 74 (n = 6) in the CP. *CBF values measured by FAIR were in good agreement with those measured by the autoradiographic ^{14}C-iodoantipyrine technique in rats (21) under conditions of anesthesia and pCO_2 identical to those of the present study* (see Table 1). It is also worth pointing out that despite the use of a surface detection coil, the CBF maps shown in Fig. 4 do not have any depth-dependent variations, in contrast to the IR and FAIR images (e.g., see Figs. 1A and 1C), since the B_1 effects are canceled out when Eq. [1] is used in the calculation of CBF.

The relationship between CBF in parietal cortex, which was calculated by FAIR, and arterial pCO_2 is shown in Fig. 5. Linear fitting of the calculated CBF on pCO_2 revealed that CBF (ml/100 g/min) = 6.07*pCO_2 (mmHg) − 137.8. The observed pCO_2 index (6.07 ml/100 g/min/mmHg) agrees with that measured by MR methods using continuous inversion (5.2 (2)), and by non-MR methods, such as Xenon washout (7.0 (22)), microspheres (5.0 (23)), and ^{14}C-butanol as an indicator (5.5 (24)). Importantly, the pCO_2 index measured by FAIR is consistent with that determined by freely diffusible iodoantipyrine with autoradiography under the same anesthesia (6.9 (21)). The low intercept in the pCO_2 versus CBF regression may be caused by anesthesia and an

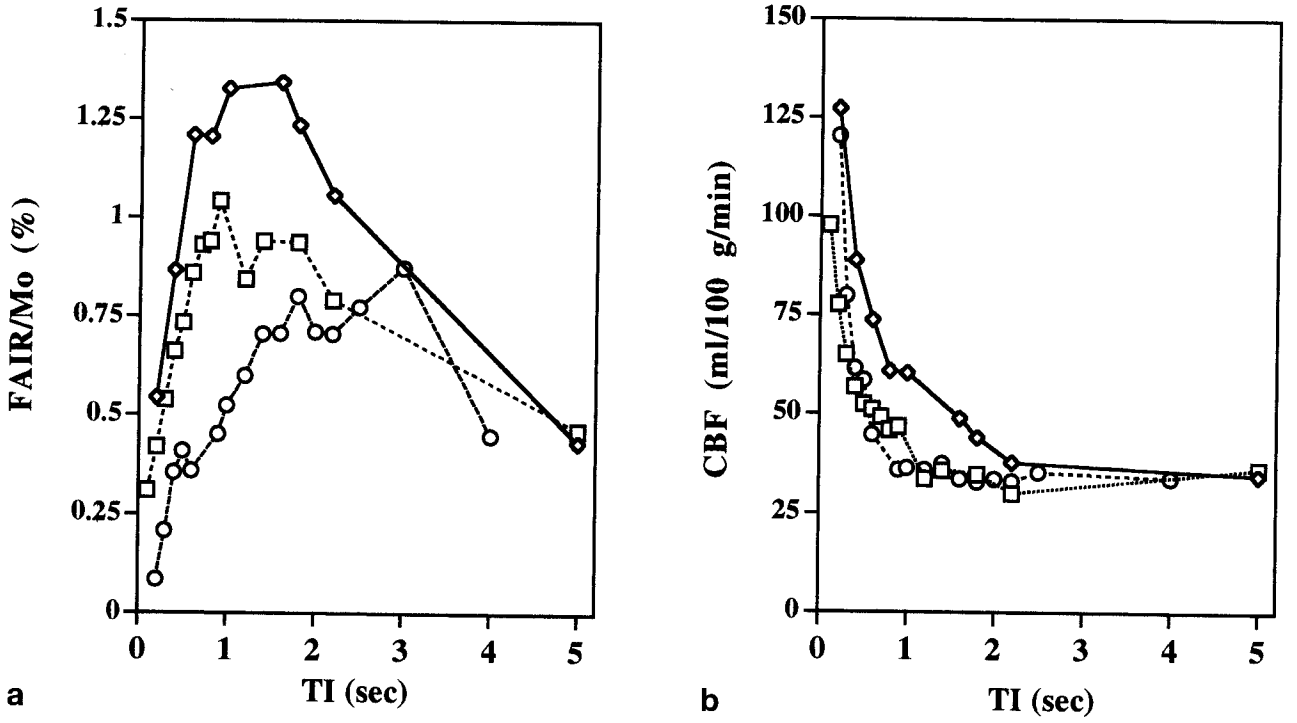

FIG. 3. TI dependence of the normalized FAIR signal (A) and the corresponding calculated CBF (B) from three representative animals. Data from the animal shown in Fig. 2 are shown as rectangles. The ROI was placed on the cortex. Large vessels were not included in the ROI. The FAIR signal was normalized relative to the thermal equilibrium magnetization. CBF was calculated by using Eq. [1].

intrinsic dependence of CBF on pCO_2. Since the vasoconstriction and vasodilation mechanisms saturate at pCO_2 levels less than 20 mmHg and greater than 80 mmHg, respectively, the functional relationship between the CBF and the pCO_2 is sigmoidal. Thus, a negative intercept can be observed.

FAIR and Focal Cerebral Ischemia

In Fig. 6, the effects of proximal (Figs. 6A, 6B, and 6C) and distal (Figs. 6D, 6E, and 6F) occlusions of the MCA on CBF, as estimated by the FAIR technique, are shown. The ssIR images are illustrated in Figs. 6A and 6D, the corresponding FAIR images in Figs. 6B and 6E, and the CBF maps in Figs. 6C and 6F. The area of reduced perfusion (indicated by arrows on the figure) is clearly delineated as the hypointense area, on both the ssIR images and the CBF maps. As expected, proximal MCA occlusion reduced CBF both in cortex and striatum. This is because the occlusion involved the lenticulostriate arteries that supply the striatum (see ref. 17). Distal MCA occlusion reduced CBF mainly in cerebral cortex because the arterial supply of the striatum was spared. These findings clearly demonstrate that FAIR is able to detect that focal reduction in CBF produced by occlusion of the MCA.

DISCUSSION

Rat Brain Perfusion Imaging at 9.4 T

Higher magnetic fields provide higher SNR. However, increased field strengths create inherent problems such as reduced T_2 values and increased tissue susceptibility effects (with the concordant shortening of T_2*). These studies illustrate that high quality IR anatomical and FAIR images can be generated by using the gradient-recalled echo sequence with short TE.

For the quantification of CBF, T_1 and apparent T_1 (T_{1app}) can be calculated from non-slice-selective and slice-selective IR images, respectively (8, 9). Then, CBF can be determined using $f/\lambda = 1/T_{1app} - 1/T_1$ (1, 2). To obtain T_1 and T_{1app} accurately, multiple IR images with *various* inversion times should be acquired. Thus, the imaging time is long. To overcome this problem, we used IR images with a *single* inversion time for the quantification of CBF (10, 14).

Effect of Blood T_1 at 9.4 T

In ssIR images, inflowing blood enters the imaging slice in the thermal equilibrium state, and thus, no blood relaxation occurs. In contrast, in the nsIR images, the blood spins recover with T_{1b}, whereas the tissue recovers with T_1. Thus, the effective $1/T_1$ will be $\rho/T_{1b} + (1 - \rho)/T_1$, where ρ is the blood volume fraction (8). The assumption is that $T_{1b} = T_1$ will induce errors in CBF calculation; in the case that $T_{1b} > T_1$, the calculated CBF without considering different T_1 values will be overestimated and its error will be higher at longer TIs. At low magnetic fields (1.5 T), errors may be as high as 20% on gray matter and 100% on white matter (8, 13). At 9.4 T, T_1 of tissue and blood gets longer and converges; T_1s of cortex and caudate putamen are 1.91 and 1.78 s, whereas T_1 of blood is 2.2 s. In the worst scenario, the fractional errors in the caudate putamen introduced by the assump-

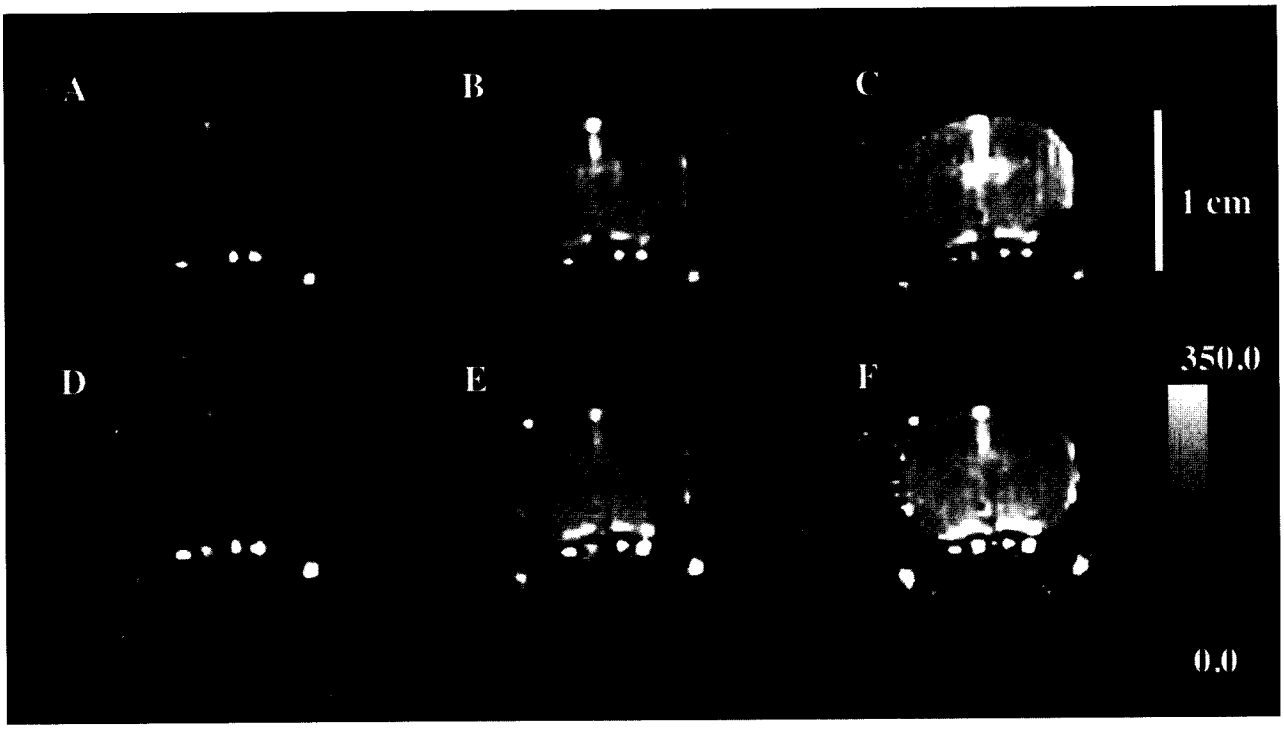

FIG. 4. Representative FAIR images (A, B, C) and the corresponding calculated CBF-maps (D, E, F) from a graded hypercapnia study, illustrating the results at hypocapnia pCO_2 = 25 mmHg (A, D), at pCO_2 = 40 mmHg (B, E), and at hypercapnia pCO_2 = 71 mmHg (C and F). A gray-scale bar indicates calculated CBF from 0 to 350 ml/100 g/min. The 1-cm distance bar is also shown.

tion $T_1 = T_{1b}$ are less than 10% and 18% at the TI of 2 and 5 s, respectively. Consequently, Eq. [1] can be used without the correction factor. However, in all of our studies, the calculated CBF was corrected for different tissue and blood T_1 relaxation rates as they were measured in this study.

TI Dependency of FAIR

The role of TI in the FAIR technique is crucial since it represents the time allowed for the tagged spins to advance into the intravascular and extravascular space. Theoretically, from Eq. [1], it is expected that the calculated CBF should be TI independent over the entire range of TI values. In the presented studies, a TI dependence of CBF at low TI values was observed, resulting in overestimation toward the shorter TI values. However, the calculated CBF was TI independent for TI > 1.5 s up to a TI of 5 s.

FAIR signal is composed mainly of two components; one is from the large arterial vascular compartment, including arteries and arterioles, and the other is from tissue/capillaries. Initially, the arterial compartment with high flow velocities will be filled first, and thus, these pixels will have higher signal enhancement in FAIR images. After filling the *macrovascular* compartments, tagged spins distribute into capillaries and subsequently exchange with the extravascular water. Beyond that time point in the evolution of the phenomenon, it is

Table 1
Comparison of CBF in Rats Measured by Noninvasive FAIR MRI and Invasive Autoradiographic Iodoantipyrine (IAP) Methods[a]

Conditions	Methods	pCO_2 (mmHg)	CBF (ml/100 g/min)
Normocapnia	FAIR	38 ± 2	91 ± 31 (n = 5)
	IAP	37 ± 1	85 ± 24 (n = 5)
Hypercapnia	FAIR	65 ± 5	243 ± 54 (n = 6)
	IAP	61 ± 2	254 ± 49 (n = 5)

[a] CBF was obtained from the parietal cortex of rats during two arterial pCO_2 levels. The same anesthesia was used for both FAIR and IAP studies (21). Values are means and their SEM.

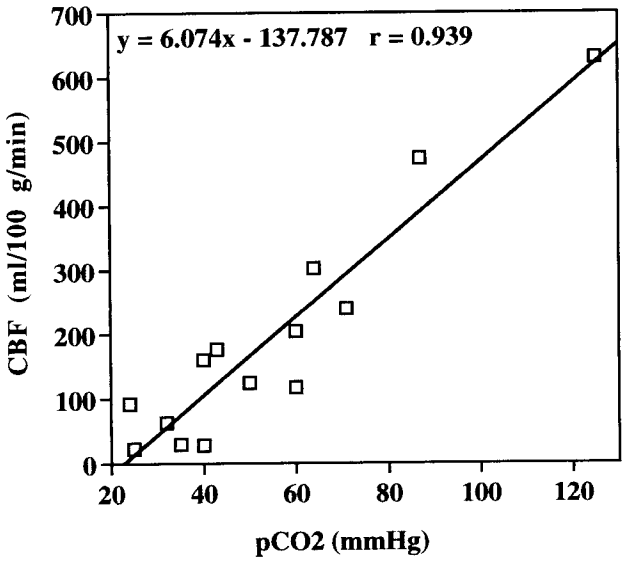

FIG. 5. The CBF, measured with the FAIR technique, at different pCO_2 levels due to graded hypercapnia from the rat brain on an ROI placed on the parietal cortex. The equation and r value with the best linear fitted line are shown.

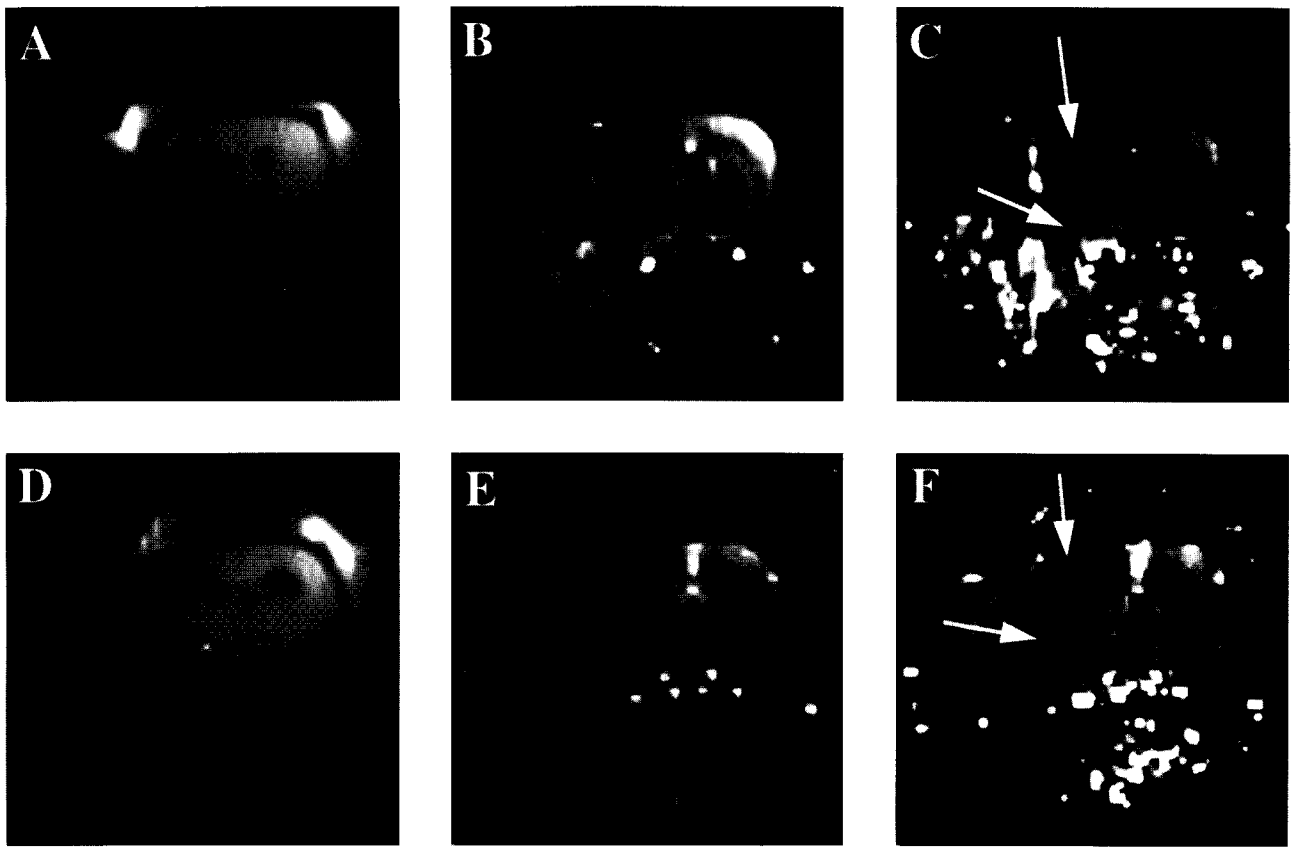

FIG. 6. IR images (A, D) and corresponding FAIR (B, E) and CBF maps (C, F) of rats subjected to proximal (A, B, C) and distal (D, E, F) occlusions of the MCA. Arrows indicate the area of reduced perfusion.

expected that the FAIR contrast is primarily sensitive to perfusion. At a much later time, tagged spins will enter the venous vessels. However, since tagged spins will be mixed completely with tissue spins in the capillary area (assuming that water is freely diffusible), very few tagged spins will exist in the venous vessels at TI < 5 s, and furthermore, the concentration of tagged spins in veins will be the same as that in tissue. Therefore, we are not concerned with the venous vessel component for our analysis. Note that large venous vessels have high FAIR contrast in some FAIR images, not because of outflow from tissue within the imaging slice, but because of inflow from outside the inversion slab. These large veins passing through the imaging slice can be identified easily since large signal intensities can be observed at short TI. We did not include large vessel areas for the ROI analysis.

At short TI, the arterial compartment contributes significantly to FAIR signal. Thus, the CBF calculated using Eq. [1] is overestimated significantly at short TI values. The relative contribution of the vascular compartment will be diminished at higher TI values, where the tissue compartment exhibits the higher signal enhancement. Considering the fact that the arterial vascular compartment is less than 1% (25), the vascular contribution will be minimal compared to the tissue/capillary contribution when TI is greater than 1.5 s. Thus, the calculated CBF was constant within the experimental error for TI > 1.5 s, suggesting that FAIR observes *microvascular/perfusion* compartments predominantly. By increasing TI, relative contribution of large vessels to FAIR signal can be further reduced. Also, longer TI values would result in measurements that are conceptually closer to what is defined as perfusion. However, spin tagging is lost by T_1 relaxation. Consequently, perfusion studies with endogenous contrast agents benefit from higher magnetic fields because of the longer T_1 values of the tissue, providing higher SNR at later TI values. To achieve maximum SNR and to reduce large vessel contributions, the TI value was set to 2.0 s for hypercapnia studies. This duration is adequate to allow the inflowing spins to distribute in the perfusion bed, especially in small animal studies, in which the blood travels shorter vessel distances.

An alternative way to remove macrovascular contribution is to use bipolar gradients (26). When spins move along the gradient direction between two gradient pulses, these spins will acquire a phase shift relative to the nonmoving spins within the pixel, resulting in signal loss. Similarly, velocity gradients across vessels and vessel tortuousness may lead to signal loss within a voxel (27). This method has been used successfully to eliminate vascular contributions (26, 28). However, it is worthwhile to mention that bipolar gradients will reduce signals not only from large vessels but also from small vessels, including capillaries (29). Although the contribution of the macrovascular compartment could be crushed, long TI values were required to ensure sufficient time for water to reach the capillaries (26).

Validation of CBF Measurements by FAIR

The present studies demonstrate that FAIR can provide absolute CBF values that are in accordance with those established by previous non-MR or MR-based methods (3, 21–24). Furthermore, resting CBF values and the increases in CBF produced by hypercapnia measured by the FAIR technique are in agreement with values measured by autoradiography in rats under the same anesthesia and comparable pCO_2 levels (21). To determine whether FAIR could also monitor decreases in CBF, we studied the hemodynamic consequences of MCA occlusion. We found that FAIR was able to delineate the ischemic area as expected on the basis of the vascular territories involved by the arterial occlusion. These observations, collectively, suggest that the FAIR technique is not only able to accurately monitor resting CBF and the increases produced by hypercapnia but also the reduction in CBF produced by focal ischemia. Therefore, the FAIR method allows measurement of CBF regionally, quantitatively, and noninvasively. This validation of CBF quantitation using the FAIR technique is independent of the magnetic field strength. However, implementation of the FAIR technique at any magnetic field would require optimization of the TI period, considering spin delivery time and T_1 relaxation.

No large vessel contributions were assumed for the CBF calculation from the FAIR signal intensity. In the CBF maps shown in Figs. 3 and 6, pixels containing large vessels were clearly shown as high CBF values; this is not desirable because there is minimal tissue/capillary blood flow. These pixels were not included for the comparison studies shown in Table 1. The ROI is placed in tissue areas primarily. At such sites, large arterial vascular contribution is expected to be minimal compared to the tissue/microvascular component based on the TI dependency studies since TI was set to 2 s. However, vascular areas were not eliminated in the ROI, and thus, CBF was overestimated. Similar experiments with bipolar gradients are necessary in future studies to determine the tissue contribution only.

We assumed that M_{ns} is flow independent. This can be satisfied when inflowing and tissue spins are in the same magnetization state when data acquisition occurs. Practically, this requires that all spins entering the imaging slice during the TI and acquisition periods have experienced the global inversion pulse. If the inversion pulse fails to invert all the inflowing spins, untagged spins in the thermal equilibrium state will enter the imaged slice at a later time. When the transit time of untagged spins is shorter than TI, this will result in reduction of the FAIR contrast, which should be included for quantification (13, 20). When the smaller *head*-volume coil (used for the blood T_1 studies) was used for FAIR studies, untagged spins from the heart and neck moved into the imaging slice during the TI, reducing FAIR contrast and underestimating CBF (data not shown). To satisfy the assumption that the nsIR image is flow independent, a *body*-volume coil covering the animal up to the level of the abdomen was used in these studies.

It is assumed that signal intensities of nsIR images are identical during normocapnia and hypercapnia conditions. As described in the Effect of Blood T_1 at 9.4 T section, the effective T_1 in nsIR images is dependent on the blood volume fraction. Since the blood volume fraction will increase when pCO_2 levels increase, the effective T_1 will increase too. Consequently, the measured CBF may be overestimated without considering this effect. For example, when the blood volume fraction increases from 5% to 7.5% in the parietal cortex, the effective T_1 of nsIR images will increase by 0.006 s, resulting in 1% signal increase of the nsIR image at TI of 2 s. This will not induce significant changes in the CBF calculation and was not considered in this study.

We assumed that tagged spins are delivered into capillaries instantaneously. In rats, the time that arterial blood travels a 5-mm distance is less than 200 ms (see Fig. 3) (3). Errors introduced by neglecting the mean transit times will be small in rats. However, especially in humans, the mean transit time of gray matter area is 0.9 s (26) and should be included in the analysis. Without considering the mean transit time, calculated CBF will be underestimated.

An assumption made in deriving Eq. [1] was that the water behaves as a freely diffusible tracer; i.e., the water can freely exchange between the intravascular and extravascular space, resulting in an extraction fraction of 1.0. Whether the water is a freely diffusible tracer is an important issue that has been examined in several studies, both with MR- and with non-MR-based methods for monitoring cerebral perfusion (e.g., refs. 28–33). In particular, studies in primates using $H_2{}^{15}O$ as an exogenous tracer have shown that when the CBF exceeds 65 ml/100 g/min (33), labeled water no longer behaves as a freely diffusible tracer. In studies in rhesus monkeys (32) and rats (30), it was found that the calculated extraction fraction of water is progressively reduced at increased CBF. Similarly, measurements of CBF with deuterium NMR and the continuous inversion method have demonstrated that the labeled water cannot be considered freely diffusible above 250 ml/100 g/min (28, 29, 31). Recent studies by arterial spin tagging suggest that the extraction fraction is greater than 0.85 when CBF is less than 250 ml/100 g/min (28, 29). Thus, an extraction fraction of less than 1.0 results in underestimation of CBF. This is a potential source of error in the FAIR studies presented herein and will be the subject of future studies. However, the close correspondence between the CBF values obtained with FAIR and those obtained with iodoantipyrine, a tracer that is more diffusible than water, suggests that diffusion limitations are not a major concern for FAIR measurements when CBF of rats is less than 250 ml/100 g/min. Studies in which CBF is measured by FAIR and iodoantipyrine *in the same rats* are required to provide a more accurate comparison between these two methods.

In the presented studies, the FAIR technique was implemented in a single-slice mode. However, multislice implementation of the FAIR technique is essential for assessment of perfusion on the entire brain. Multislice FAIR imaging can be accomplished in a conventional manner, as used here, by acquisition of multiple single slices using a gradient-recalled echo technique. However, such an approach requires a long time to acquire

many slices with adequate SNR. A more advanced method for multislice imaging is the combined use of multislice FAIR and echo-planar imaging acquisition, in which multiple slices can be acquired after a single inversion pulse (11).

CONCLUSION

The FAIR technique was implemented at 9.4 T to assess rat brain perfusion using the blood water as an endogenous contrast agent. To obtain a perfusion component in FAIR images, the TI should be greater than 1.5 s. At high magnetic fields, the SNR at a given TI is higher because of longer T_1 values. FAIR was found to provide CBF values that correspond well to those obtained with other methods, both in the resting state and during the cerebrovasodilation produced by graded levels of hypercapnia. Furthermore, FAIR was able to accurately detect the spatial distribution of the reduction in CBF produced by occlusion of the rat MCA. FAIR, therefore, is a useful technique in the study of cerebral hemodynamics both in the normal state and in cerebral ischemia.

ACKNOWLEDGMENTS

The authors thank Joseph Sikora for helping with experiments and Marlene Merscher for critical readings of the manuscript.

REFERENCES

1. J. A. Detre, J. S. Leigh, D. S. Williams, A. P. Koretsky, Perfusion imaging. *Magn. Reson. Med.* **23,** 37–45 (1992).
2. D. S. Williams, J. A. Detre, J. S. Leigh, A. P. Koretsky, Magnetic resonance imaging of perfusion using spin inversion of arterial water. *Proc. Natl. Acad. Sci. U S A* **89,** 212–216 (1992).
3. W. Zhang, D. S. Williams, J. A. Detre, A. P. Koretsky, Measurement of brain perfusion by volume-localized NMR spectroscopy using inversion of arterial water spins: accounting for transit time and cross-relaxation. *Magn. Reson. Med.* **25,** 362–371 (1992).
4. D. A. Roberts, J. A. Detre, L. Bolinger, E. K. Insko, J. S. Leigh, Quantitative magnetic resonance imaging of human brain perfusion at 1.5T using steady-state inversion of arterial water. *Proc. Natl. Acad. Sci. U S A* **91,** 33–37 (1994).
5. W. Zhang, A. Silva, D. Williams, A. Korestsky, NMR measurement of perfusion using arterial spin labeling without saturation of macromolecular spins. *Magn. Reson. Med.* **33,** 370–376 (1995).
6. R. R. Edelman, B. Siewert, D. G. Darby, V. Thangaraj, A. C. Nobre, M. M. Mesulam, S. Warach, Qualitative mapping of cerebral blood flow and functional localization with echo-planar MR imaging and signal targeting with alternating radio frequency. *Radiology* **192,** 513–520 (1994).
7. S.-G. Kim, Quantification of relative cerebral blood flow change by flow-sensitive alternating inversion recovery (FAIR) technique: application to functional mapping. *Magn. Reson. Med.* **34,** 293–301 (1995).
8. K. K. Kwong, D. A. Chesler, R. M. Weisskoff, K. M. Donahue, T. L. Davis, L. Ostergaard, T. A. Campbell, B. R. Rosen, MR perfusion studies with T_1-weighted echo planar imaging. *Magn. Reson. Med.* **34,** 878–887 (1995).
9. C. Schwarzbauer, S. Morrissey, A. Haase, Quantitative magnetic resonance imaging of perfusion using magnetic labeling of water proton spins within the detection slice. *Magn. Reson. Med.* **35,** 540–546 (1996).
10. S.-G. Kim, K. Ugurbil, Comparison of blood oxygenation and cerebral blood flow effects in fMRI: estimation of relative oxygen consumption change. *Magn. Reson. Med.* **38,** 59–65 (1997).
11. S.-G. Kim, N. V. Tsekos, J. Ashe, Multi-slice perfusion-based functional MRI using the FAIR technique: comparison of CBF and BOLD effects. *NMR Biomed.* **10,** 18–24 (1997).
12. S.-G. Kim, N. V. Tsekos, Perfusion imaging by a flow-sensitive alternating inversion recovery (FAIR) technique: application to functional brain imaging. *Magn. Reson. Med.* **37,** 425–435 (1997).
13. F. Calamante, S. Williams, N. van Bruggen, K. Kwong, R. Turner, A model for quantification of perfusion in pulsed labelling techniques. *NMR Biomed.* **8,** 79–83 (1996).
14. R. Buxton, E. Wong, L. Frank, Quantitation issues in perfusion measurements with dynamic arterial spin labeling, *in* "Proc., ISMRM, 4th Annual Meeting, New York, 1996," p. 10.
15. P. Herscovitch, M. E. Raichle, What is the correct value for the brain-blood partition coefficient for water? *J. Cereb. Blood Flow Metab.* **5,** 65–69 (1985).
16. M. Garwood, K. Ugurbil, B1 insensitive adiabatic RF pulses. *NMR Basic Prin. Prog.* **26,** 110–147 (1992).
17. F. Zhang, C. Iadecola, Stimulation of the fastigial nucleus enhances EEG recovery and reduced tissue damage after focal cerebral ischemia. *J. Cereb. Blood Flow Metab.* **12,** 962–970 (1992).
18. J. P. Strupp, Stimulate: a GUI based fMRI analysis software package. *NeuroImage* **3,** S607 (1996).
19. S.-G. Kim, X. Hu, K. Ugurbil, Accurate T_1 determination from inversion recovery images: application to human brain at 4 tesla. *Magn. Reson. Med.* **31,** 445–449 (1994).
20. N. V. Tsekos, K. Ugurbil, S.-G. Kim, Effect of sequence parameters in assessment of tissue perfusion, *in* "Proc., ISMRM, 4th Annual Meeting, New York, 1996," p. 1310.
21. C. Iadecola, X. Xu, Nitro-L-arginine attenuates hypercapnic cerebrovasodilation without affecting cerebral metabolism. *Am. J. Physiol.* **266,** R518–R525 (1994).
22. B. Eklof, N. A. Lassen, L. Nilsson, K. Norberg, B. K. Seisjo, P. Tarlof, Regional cerebral blood flow in the rat measured by the tissue sampling techniques; a critical evaluation using four indicators C^{14}-antipyrine, C^{14}-ethanol, H^3-water, and $Xenon^{133}$. *Acta. Physiol. Scand.* **91,** 1–10 (1974).
23. S. Mori, A. C. Ngai, K. R. Ko, H. R. Winn, A venous outflow method for continuously monitoring cerebral blood flow in the rat. *Am. J. Physiol.* **250,** H304–H312 (1986).
24. R. P. Shockley, J. C. LaManna, Determination of rat cortical blood volume changes by capillary mean transit time analysis during hypoxia, hypercapnia and hyperventilation. *Brain Res.* **454,** 170–178 (1988).
25. K. C. Hodde, *in* "The Cerebral Veins: An Experimental and Clinical Update" (L. M. Aver, F. Loew, Eds.), pp. 85–92, Springer-Verlag, New York, 1983.
26. F. Q. Ye, V. S. Mattay, P. Jezzard, J. A. Frank, D. R. Weinberger, A. C. McLaughlin, Correction for vascular artifacts in cerebral blood flow values by using arterial spin tagging techniques. *Magn. Reson. Med.* **37,** 226–235 (1997).
27. D. Le Bihan, E. Breton, D. Lallemand, P. Grenier, E. Cabanis, M. Laval-Jeantet, MR imaging of intravoxel incoherent motions: application to diffusion and perfusion in neurologic disorders. *Radiology* **161,** 401–407 (1986).
28. A. C. Silva, W. Zhang, D. S. Williams, A. P. Koretsky, Estimation of water extraction fractions in rat brain using magnetic resonance measurement of perfusion with arterial spin labeling. *Magn. Reson. Med.* **37,** 58–68 (1997).
29. A. C. Silva, D. S. Williams, A. P. Koretsky, Evidence for the exchange of arterial spin-labeled water with tissue water in rat brain from diffusion sensitized measurements of perfusion. *Magn. Reson. Med.* **38,** 232–237 (1997).
30. K. Gwan Go, A. A. Lammertsma, A. M. J. Paans, W. Vaalburg, M. G. Woldring, Extraction of water labeled with oxygen 15 during single capillary transit. *Arch. Neurol.* **38,** 581–584 (1981).
31. R. J. T. Corbett, A. P. Laptook, E. Olivares, Simultaneous measurement of cerebral blood flow and energy metabolites in piglets using deuterium and phosphorus nuclear magnetic resonance. *J. Cereb. Blood Flow Metab.* **11,** 55–65 (1991).
32. J. O. Eichling, M. E. Raichle, J. R. L. Grubb, M. M. Ter-Pogossian, Evidence of the limitations of water as a freely diffusible tracer in brain of the Rhesus monkey. *Circ. Res.* **35,** 358–364 (1974).
33. M. E. Raichle, W. R. W. Martin, P. Herschcovitch, M. A. Mintun, J. Markham, Brain blood flow measured with intravenous $H_2{}^{15}O$. II. Implementation and validation. *J. Nucl. Med.* **24,** 790–798 (1983).